Research Square

Preprints are preliminary reports that have not undergone peer review.
They should not be considered conclusive, used to inform clinical practice,
or referenced by the media as validated information.

Ocean Greening Amid Warming: Evidence from Stringently-screened Ocean Color Data

Shaoling Shang

slshang@xmu.edu.cn

State Key Laboratory of Marine Environmental Science, College of Ocean and Earth Sciences, Xiamen University https://orcid.org/0000-0001-8109-9468

Longteng Zhao

State Key Laboratory of Marine Environmental Science, College of Ocean and Earth Sciences, Xiamen University

Xiaolong Yu

Xiamen University https://orcid.org/0000-0003-2813-0854

Shuaixing Peng

State Key Laboratory of Marine Environmental Science, College of Ocean and Earth Sciences, Xiamen University https://orcid.org/0009-0006-9794-3284

Zhongping Lee

Xiamen University

Wei-Lei Wang

Xiamen University https://orcid.org/0000-0002-3201-7224

Xiaomin Ye

National Satellite Ocean Application Service (NSOAS), Key Laboratory of Space Ocean Remote Sensing and Application, Ministry of Natural Resources

Xin Liu

State Key Laboratory of Marine Environmental Science, Xiamen University https://orcid.org/0000-0002-7925-9618

Peng Xiu

Xiamen University https://orcid.org/0000-0001-5328-8405

Dalin Shi

Xiamen University https://orcid.org/0000-0003-4432-1992

Minhan Dai

Xiamen University https://orcid.org/0000-0003-0550-0701

Article

Keywords:

Posted Date: March 3rd, 2026

DOI: https://doi.org/10.21203/rs.3.rs-8978653/v1

License: This work is licensed under a Creative Commons Attribution 4.0 International License.
Read Full License

Additional Declarations: There is **NO** Competing Interest.

Abstract

The subtlety of oceanic color shifts, compounded by noise in satellite records, has made it uncertain whether the open ocean is undergoing a change akin to terrestrial greening. Using optical indices derived from a new, stringently screened MODIS-Aqua remote sensing reflectance dataset, we show that the ocean (60° S–60° N) has become markedly greener over the past two decades, with 73% of latitudinal bands exhibiting a shift toward greener hues and 24% showing statistically significant trends. By separating optical signals from different constituents, we attribute this greening primarily to increases in phytoplankton pigments, accompanied by smaller increases in other optically active components. We suggest the observed greening results from a complex interplay of warming-driven competitive advantages of picophytoplankton, mixed layer dynamics and atmospheric dust deposition. Importantly, we find that previously perceived chlorophyll-a concentration (Chl) decline in mid-low latitudes (40° S–40° N) are largely driven by radiance data of lower-certainty; removing these data reverses the trend. Moreover, the water corresponding to these data is not warming, further challenging the conventional causal mechanism that links warming to reduced Chl. Collectively, these results reveal that Earth's largest biome is undergoing a subtle yet detectable greening in response to climate change.

Introduction

In the context of climate change, the era of ocean color satellites has heightened scientific and public awareness of changes in the global ocean ecosystem, with key focuses including shifts in chlorophyll-a concentration (Chl)[1–3], phytoplankton biomass and primary production[4–6], the dynamics of ecologically significant ocean regions[7,8], and coastal phytoplankton blooms[9,10]. The mainstream perspective posits that global warming induces enhanced stratification, which in turn limits nutrient supply from depth, leading to a reduction in Chl levels and primary production. Recent attention has turned to the color changes of the ocean[9,11–13], partly inspired by discussions of earth greening—the increasing trend in land vegetation driven by climate change and human activities[14–17]. For example, it is suggested that the ocean as a whole is becoming greener, based on the observation that increases in the remote sensing reflectance (R_{rs})—a measure of ocean's color spectrum—of the green wavelengths occur more frequently than decreases[11]. Another new perspective indicates that the blue ocean areas are becoming bluer, marked by a decreasing trend in satellite-derived Chl, concurrent with a poleward greening, signaled by increasing Chl[12].

As such, the nature of the color changes in the ocean remains a subject of ongoing debate, primarily stemming from two key factors. First, the ocean's color is fundamentally determined by the relative intensity of water's radiance (or R_{rs}) across the red, green, and blue spectral bands (Fig. S1). Chl, a biogeochemical index of phytoplankton biomass, is only a proxy for the ocean's color rather than a direct optical measurement of the color itself. Second, uncertainties persist regarding satellite R_{rs} measurements and their products, such as Chl[18–20]. Caution is warranted because the rate of oceanic

changes is often less than 1% per decade[21–23], making its detection and interpretation highly sensitive to data quality.

Furthermore, previous works have primarily focused on phytoplankton as the determinant of ocean color, overlooking the role of other optically active constituents (OACs) that may dominate ocean color signals for the blue wavelengths (Fig. S1). Understanding what drives oceanic color changes requires assessing the respective contributions of different materials, which necessitates distinguishing the optical signals of phytoplankton pigments from other OACs.

Therefore, using direct and highest-quality spectral measurements of ocean color is crucial to the investigation of oceanic color shifts and their attribution to phytoplankton versus other OACs. Here we present a new analysis of hue angle, which is an intuitive and direct index describing color (Fig. S1, also see Methods), using a rigorously screened R_{rs} dataset from the Moderate Resolution Imaging Spectroradiometer on the Aqua satellite (MODIS-Aqua; hereafter MODIS). This dataset was generated by an up-to-date quality-assurance framework that applies two stringent spectral criteria to further screen NASA-flagged high-quality data, thereby enabling the selection of the highest-quality (HQ) MODIS R_{rs} data in the broad expanse of oceanic waters (see methods)[24]. Further, to disentangle the contributions of phytoplankton pigments from other OACs to the observed color changes, we calculated key optical indices of OACs—the absorption coefficients at 443 nm of phytoplankton ($a_{ph}(443)$) and that of color dissolved organic matter and particulate detritus (hereafter nonliving materials for simplicity) ($a_{dg}(443)$) (see methods). We aim to rigorously evaluate and interpret the color changes in the ocean across 60° S–60° N over the past two decades, with a specific focus on open ocean regions, i.e., clear oceanic waters beyond the continental shelf (excluding data of depth < 200 m).

Results

Latitudinal trends of hue angle, the absorption coefficients of phytoplankton and nonliving materials

The HQ R_{rs} data between 60° S and 60° N (38%–82% of NASA's standard R_{rs} data (Fig. 1a)) were used to calculate the climatology of hue angle from January 2003 to December 2022 and the annual mean hue angle of each 1° latitudinal band. Globally, the 20-year mean hue angle falls between 188° and 238°. The bluest waters (hue angles > ~ 220°) are located in the subtropical gyres, as shown in Fig. 1b. Trends in hue angle were then determined using the non-parametric Mann-Kendall (M-K) test for significance, with the magnitude of any significant trend quantified by Sen's slope estimator (see methods). Interestingly, as Fig. 1c shows, a decreasing trend of hue angle, suggesting greening, is found for 73% of the latitudinal bands between 60° S and 60° N, of which 24% are statistically significant ($P < 0.05$). Within the mid-low latitudes (40° S–40° N), where a bluer trend was reported based on standard MODIS Chl products[12], 65% of the latitudinal bands show a greening trend. Most of these greening bands are

concentrated in the Southern Hemisphere. In contrast, weak and non-significant trends toward bluer oceans (increasing hue angle) are found primarily in the Northern Hemisphere's subtropical gyres.

Overall, using the premium quality MODIS R_{rs} data, we demonstrate a greening of the ocean between 60° S and 60° N from 2003 to 2022. This greening could result from an increase in OACs, since the increase in these constituents will lead to enhanced absorption at the blue wavelengths, which will then shift ocean color to greener. Indeed, we found that 56% of the latitudinal bands exhibit an increasing trend in $a_{ph}(443)$ (Fig. 1d), the main light absorber in the blue domain. Meanwhile, an increasing trend of $a_{dg}(443)$ was also observed for 58% of the latitudinal bands (Fig. 1e). These results indicate that both phytoplankton pigments and nonliving materials contribute to ocean greening, with phytoplankton pigments (an index of Chl) playing the dominant role—its rate of increase is approximately three times that of nonliving materials.

Relationship of color changes with warming

While the hue angle trend exhibits a distinct spatial pattern across latitudes, the spatial mean of hue angle for the entire basin (60° S–60° N) itself also shows a significant decreasing trend in 2003–2022, accompanied by a significant warming trend (Fig. 1f, $P < 0.05$), suggesting that the global ocean is turning greener while sea surface temperature (SST) rises. Concurrent significant increasing trends in the spatial means of $a_{ph}(443)$ and $a_{dg}(443)$ further offer a plausible explanation of the observed greening trend (Fig. 1g). Spatial mean analysis of hue angle, absorption coefficients, and SST for the mid-low latitudes (40° S–40° N)—a region reported to have bluer trends based on NASA's standard Chl products[12]—revealed consistent greening-warming coupled trends (Fig. S2).

Taken together, strictly quality-assured MODIS R_{rs} data between 60° S and 60° N provide a new insight that warming is accompanied by a greening trend in the ocean during 2003–2022. Such a greening trend is found chiefly due to an increase in phytoplankton pigments (signified by increasing $a_{ph}(443)$), with minor contribution from nonliving materials (signified by increasing $a_{dg}(443)$).

Discussion

The greening trend we observed is consistent with historical studies of 40° – 60° latitude waters, where increased temperature have been reported to enhance phytoplankton growth in these cooler oceanic regions via various dynamic and physiological processes[25,26]. The results for the mid-low latitude waters (40° S–40° N), however, contradict earlier observations that were primarily based on standard Chl products from different satellites with varying temporal coverages[1–3,27]. Hereafter, for a comprehensive comparison of warming-driven color changes with prior studies, we examine the relationship of warming with Chl, a product that inherently represents a combined signal of $a_{ph}(443)$ and $a_{dg}(443)$[28,29].

Indeed, our analysis of standard MODIS Chl and SST data during 2003–2022 also reveals a similar significant decreasing trend in Chl and an inverse Chl-SST relationship in the mid-low latitudes (40° S–40° N) (Fig. 2, black lines). The Chl derived from HQ R_{rs} data with the same retrieval algorithm[20,30,31], however, exhibits a significant increasing trend, a pattern that aligns with the consistent changes observed in hue angle, $a_{ph}(443)$ and $a_{dg}(443)$, and coincides with rising SST across 40° S–40° N (Fig. 2, red lines). What mechanisms, then, could explain the observed increasing Chl in this warm, permanently stratified ocean, where picophytoplankton mostly dominate? An initial line of support comes from an inference that warmer ocean conditions can lead to elevated picophytoplankton biomass[32]. This inference is drawn from an analysis of a global abundance dataset and is grounded in the observed competitive advantages for picophytoplanktons with high ratios of surface-area *vs.* volume and low nutrient requirements[33,34]. Furthermore, a recent exploration of an extensive global field dataset reveals a paradoxical trend: despite the widely documented intensification of ocean stratification under global warming[5,35–37], the summer mixed layer actually deepened at a rate of 2.9% (± 0.5%) per decade (typically 5–10 m) from 1970 to 2018, rather than a shallower mixed layer typically expected[21]. Mixed layer deepening thereby either increases phytoplankton biomass by enhancing nutrient availability or leads to higher Chl via photoacclimation[4,38].

On the other hand, while our analysis reveals an overall greening across 60° S–60° N, spatial heterogeneity exists. The southern hemisphere shows more pronounced greening than the northern hemisphere (85% *vs.* 63% of latitudinal bands), which aligns with reported strengthening of the Southern Hemisphere Westerlies[39,40], since stronger winds promote deeper mixing and thus higher OACs. Meanwhile, lidar measurements reveal an increasing trend in dust deposition over the southern hemisphere during the past two decades[41], which could further explain the enhanced greening observed there, as increased iron supply from dust can alleviate iron limitation and stimulate phytoplankton growth[42]. In contrast, bluing regions are primarily concentrated in the North Pacific Subtropical Gyre (NPSG, 57% of the latitudinal bands in 20° N–40° N of the Pacific are significantly bluer). This could result from regional variation in how MLD responds to warming, since MLD shoaling—which can reduce Chl—is evident in the North Pacific[21].

Additionally, we examined the Chl derived solely from non-HQ R_{rs} data (~ 30% of the standard data, spatially widespread), finding a significant decreasing trend (Fig. 2a, brown lines). It thus suggests that the overall decreasing trend in Chl derived from standard MODIS R_{rs} is driven by the filtered-out non-HQ R_{rs} data, which are associated with higher uncertainties. This striking contrast between the Chl trends derived from HQ and non-HQ R_{rs} data implies that the direction of oceanic shifts can be reversed with ~ 30% data, a portion that does not meet the highest-quality criteria. Importantly, however, SST corresponding to these non-HQ R_{rs} data exhibits a slight, non-significant decrease (Fig. 2b, brown lines). This means the observed Chl decline in this subset—even if real—is decoupled from warming, thereby challenging the conventional causal mechanism that links warming to reduced Chl via enhanced stratification and nutrient limitation.

Altogether, by implementing a strict quality control strategy for satellite ocean color data, our study reveals a coherent, large-scale greening trend in the ocean across 60° S–60° N. This trend is predominantly driven by enhanced phytoplankton pigment absorption, a response to warming-associated elevation in picophytoplankton alongside variations in nutrient and light availability. Our finding challenges the prevailing narrative of ocean desertification under sustained warming, suggesting that pelagic ecosystems are more dynamic and productive than previously recognized. It is important to note, however, that these global-scale signals may mask substantial regional variability in both patterns and underlying mechanisms, underscoring the necessity of integrating local processes into projections of future oceanic changes.

Moreover, the greening trend in the ocean implies potentially substantial positive effects, including enhancements to fishery yields, increased drawdown of anthropogenic CO_2, and a subsequent climate cooling feedback. Crucially, these findings in the open ocean, alongside established greening trends on land[15] and the expansion of coastal blooms[43], point to a coordinated biospheric response to global change drivers. Consequently, our work necessitates a revision of historical ocean color trends and underscores the urgency of integrating the highest-quality observations to correctly decipher the resilience and metabolic shifts of Earth's largest ecosystem.

Methods

Global monthly composite standard data products of remote sensing reflectance (R_{rs}), chlorophyll-a concentration (Chl), and sea surface temperature (SST) at 4-km resolution from Aqua satellite (MODIS-Aqua; hereafter MODIS), which covers the 20-year period from January 2003 to December 2022, were obtained from NASA's Ocean Biology Distributed Active Archive Center (OB.DAAC).

The stringent data screening framework was applied to the standard R_{rs} dataset, yielding the highest-quality (HQ) R_{rs} dataset[24]. Briefly, this framework identifies R_{rs} spectra of the lowest uncertainty through two strict spectrum-level constraints applied on top of the standard Level-2 flags (https://oceancolor.gsfc.nasa.gov/atbd/ocl2flags/). First, only R_{rs} spectra that perfectly match an *in situ* baseline database (quality assurance (QA) score of 1.0) are retained[44]. Second, for a key optical property —the total absorption coefficient—derived from R_{rs}, results from independent band-difference and band-ratio algorithms are compared[28,45]. Since the band-difference algorithm is insensitive to residual errors in R_{rs}, while the band-ratio one is highly sensitive, consistent derivatives from both algorithms indicate the highest-quality R_{rs} spectrum. A criterion is therefore proposed: R_{rs} spectra are retained only if the difference between the outputs from the two algorithms is less than 15%[24]. Note that this criterion is valid primarily for waters of Chl < ~ 1 mg/m^3, which cover about 91% of the global ocean. Also, we choose to focus on the ocean, with the R_{rs} data in shallow waters (depth < 200 m, ETOPO 2022 bathymetry) excluded.

The proportion of HQ R_{rs} is low in the high latitudes (poleward of 60°), mainly due to failures in atmospheric correction resulted from high solar zenith angles and frequent cloud cover[46,47]. We therefore define our study area as the ocean between 60° S and 60° N, where the HQ R_{rs} data account for 62% of the standard MODIS R_{rs} dataset and are distributed throughout the entire region. Moreover, within this latitudinal range, HQ data are particularly abundant in the mid-low latitudes (40° S–40° N), constituting 68% of the corresponding standard MODIS R_{rs} subset.

Using this HQ R_{rs} dataset, we calculated the hue angle based on the CIE colorimetric system (Fig. S1b)[48,49]. Unlike the human eye or broadband sensors (e.g., Landsat) that capture light in broad red, green, and blue channels, MODIS measures ocean color in discrete, narrow spectral bands (Fig. S1c). To adapt the multispectral MODIS data for CIE coordinates and minimize spectral noise, we aggregated adjacent MODIS bands to approximate broad tristimulus components. Specifically, the blue (B) component was derived by averaging R_{rs} at 443 and 488 nm; the green (G) component from 531 and 547 nm; and the red (R) component from 667 and 678 nm. These aggregated components were then converted into XYZ tristimulus values:

$$R = \left(Rrs\left(667\right) + Rrs\left(678\right)\right)/2 \left(1\right)$$

$$G = \left(Rrs\left(531\right) + Rrs\left(547\right)\right)/2 \left(2\right)$$

$$B = \left(Rrs\left(443\right) + Rrs\left(488\right)\right)/2 \left(3\right)$$

$$X = 2.7689R + 1.7517G + 1.1302B \left(4\right)$$

$$Y = 1.0000R + 4.5907G + 0.0601B \left(5\right)$$

$$Z = 0.0565G + 5.5943B \left(6\right)$$

The chromaticity coordinates (x, y) were then converted from the three tristimulus values:

$$x = \frac{X}{X+Y+Z} \left(7\right)$$

$$y = \frac{Y}{X+Y+Z} \left(8\right)$$

and were further transformed to a polar coordinate system relative to the white point $(\frac{1}{3}, \frac{1}{3})$. Finally, the hue angle was calculated as $hueangle = atan2(y\prime, x\prime)$(degree) with the transformed coordinates defined as $(x', y') = (x - \frac{1}{3}, y - \frac{1}{3})$ (Fig. S1b).

In addition to hue angle, the absorption coefficients of OACs were calculated. It is based on the consideration that the magnitude and spectral shape of the R_{rs}, which together determine the ocean's color, are governed by the absorption and backscattering properties of the optically active constituents (OACs) in the ocean. The OACs include phytoplankton pigments (chlorophyll-a and minor accessory pigments) and nonliving materials (color dissolved organic matter (CDOM) and particulate detritus) (Fig.

S1a & d). Standard satellite retrievals of Chl inherently incorporate both living and non-living materials, representing the collective absorption of all OACs in the water[28,29]. An effective approach to separate phytoplankton from other optical constituents is to estimate absorption contribution of various OACs individually[50,51]. We therefore derived the absorption coefficients at 443 nm for phytoplankton ($a_{ph}(443)$) and nonliving materials ($a_{dg}(443)$) from HQ R_{rs} following the widely used Quasi-Analytical Algorithm (QAA_V6)[52,53]. The 443 nm MODIS band is selected as it matches the peak absorption wavelength of chlorophyll-a, which is the principal photosynthetic pigment in phytoplankton.

To facilitate a comparative discussion with findings from previous reports based on standard Chl products, here we also derived Chl from HQ and non-HQ R_{rs} using the standard NASA hybrid algorithm (OCI)[20,30,31] employed in the R2022.0 global reprocessing, respectively. Their co-located SST were retrieved from the standard SST dataset for further analysis of their respective Chl-SST relationship (see Results).

Trend analysis was carried out by employing the non-parametric Mann-Kendall (M-K) test coupled with the Sen's slope estimator[54,55]. The M-K test was selected over simple linear regression due to its robustness against outliers and its ability to handle non-normally distributed geophysical data without requiring temporal interpolation for missing values[56]. Trends were considered statistically significant at the 95% confidence level ($P < 0.05$). Meanwhile, we considered the trade-off between data quality and quantity. The rigorous HQ screening framework, while ensuring high spectral fidelity, inevitably reduces the number of R_{rs} observations in certain regions. We thus opted for the M-K test on 1° latitudinal bands and basin-wide means, a common approach in climate and geoscience[12,27], to mitigate the impact of localized data gaps and ensure the statistical confidence of the derived trends.

Declarations

Declaration of Competing Interest

The authors declare that they have no conflict of interest.

References

1. Groom S et al (2019) Satellite ocean colour: current status and future perspective. Front Mar Sci 6:485
2. Boyce DG, Lewis MR, Worm B (2010) Global phytoplankton decline over the past century. Nature 466:591–596
3. Gregg WW, Rousseaux CS (2014) Decadal trends in global pelagic ocean chlorophyll: A new assessment integrating multiple satellites, in situ data, and models. J Geophys Res -Oceans 119:5921–5933

4. Behrenfeld MJ et al (2016) Revaluating ocean warming impacts on global phytoplankton. Nat Clim Chang 6:323–330
5. Silsbe GM, Fox J, Westberry TK, Halsey KH (2025) Global declines in net primary production in the ocean color era. Nat Commun 16:5821
6. Volta C, Bellacicco M, Xing X, Yang G, Marullo S (2024) Phytoplankton dynamics in subtropical gyres: New insights into biomass and physiology from 25 Years of satellite observations. *Geophys. Res. Lett.* 52, eGL111817 (2025)
7. Polovina JJ, Howell EA, Abecassis M (2008) Ocean's least productive waters are expanding. Geophys Res Lett 35:L03618
8. Peng S et al (2025) Ocean’s largest chlorophyll-rich tongue is extending westward (2002–2022). Nat Commun 16:103
9. Hong Z et al (2025) Declining ocean greenness and phytoplankton blooms in low to mid-latitudes under a warming climate. Sci Adv 11:eadx4857
10. Dai M et al (2023) Persistent eutrophication and hypoxia in the coastal ocean. Camb Prism Coast Futur 1:e19
11. Cael B, Bisson K, Boss E, Dutkiewicz S, Henson S (2023) Global climate-change trends detected in indicators of ocean ecology. Nature 619:551–554
12. Zhao H, Manizza M, Lozier MS, Cassar N (2025) Greener green and bluer blue: Ocean poleward greening over the past two decades. Science 388:1337–1340
13. Li Z et al (2024) Ocean-scale patterns of environment and climate changes driving global marine phytoplankton biomass dynamics. Sci Adv 10:eadm7556
14. Myneni RB, Keeling CD, Tucker CJ, Asrar G, Nemani RR (1997) Increased plant growth in the northern high latitudes from 1981 to 1991. Nature 386:698–702
15. Zhu Z et al (2016) Greening of the Earth and its drivers. Nat Clim Chang 6:791–795
16. Chen C et al (2019) China and India lead in greening of the world through land-use management. Nat Sustain 2:122–129
17. Piao S et al (2020) Characteristics, drivers and feedbacks of global greening. Nat Rev Earth Environ 1:14–27
18. Pahlevan N et al (2021) ACIX-Aqua: A global assessment of atmospheric correction methods for Landsat-8 and Sentinel-2 over lakes, rivers, and coastal waters. Remote Sens Environ 258:112366
19. Hu C, Feng L, Lee Z (2013) Uncertainties of SeaWiFS and MODIS remote sensing reflectance: Implications from clear water measurements. Remote Sens Environ 133:168–182
20. Hu CM, Lee Z, Franz B (2012) Chlorophyll a algorithms for oligotrophic oceans: A novel approach based on three-band reflectance difference. J Geophys Res -Oceans 117:C01011
21. Sallée J-B et al (2021) Summertime increases in upper-ocean stratification and mixed-layer depth. Nature 591:592–598

22. Yang H et al (2025) Onshore intensification of subtropical western boundary currents in a warming climate. Nat Clim Chang 15:301–307
23. Zhao Y, Tao Y, Chen Y, Yan J, Zeng Z (2025) Increasing extreme winds challenge offshore wind energy resilience. Nat Commun 16:9529
24. Zhao L et al (2026) Highest quality remote sensing reflectance database compiled from 20 + years of MODIS-aqua measurements. Remote Sens Environ 334:115195
25. Yang K, Meyer A, Strutton PG, Fischer AM (2023) Global trends of fronts and chlorophyll in a warming ocean. Commun Earth Environ 4:489
26. Zhao H, Matsuoka A, Manizza M, Winter A (2022) Recent Changes of Phytoplankton Bloom Phenology in the Northern High-Latitude Oceans (2003–2020). J Geophys Res -Oceans 127, e2021JC018346
27. Siegel DA et al (2013) Regional to global assessments of phytoplankton dynamics from the SeaWiFS mission. Remote Sens Environ 135:77–91
28. Lee ZP et al (1998) An empirical algorithm for light absorption by ocean water based on color. J Geophys Res -Oceans 103:27967–27978
29. Gordon HR, Morel A (1983) Remote Assessment of Ocean Color for Interpretation of Satellite Visible Imagery: A Review. Springer-, New York
30. Hu C et al (2019) Improving Satellite Global Chlorophyll a Data Products Through Algorithm Refinement and Data Recovery. J Geophys Res -Oceans 124:1524–1543
31. O'Reilly JE et al (1998) Ocean color chlorophyll algorithms for SeaWiFS. J Geophys Res -Oceans 103:24937–24953
32. Flombaum P, Wang W-L, Primeau FW, Martiny AC (2020) Global picophytoplankton niche partitioning predicts overall positive response to ocean warming. Nat Geosci 13:116–120
33. Agawin NS, Duarte CM, Agustí S (2000) Nutrient and temperature control of the contribution of picoplankton to phytoplankton biomass and production. Limnol Oceanogr 45:591–600
34. Marañón E (2015) Cell size as a key determinant of phytoplankton metabolism and community structure. Annu Rev Mar Sci 7:241–264
35. Li G et al (2020) Increasing ocean stratification over the past half-century. Nat Clim Chang 10:1116–1123
36. Li S et al (2020) The Pacific Decadal Oscillation less predictable under greenhouse warming. Nat Clim Chang 10:30–34
37. Cheng L et al (2025) Ocean stratification in a warming climate. Nat Rev Earth Environ, 1–19
38. Diaz BP et al (2021) Seasonal mixed layer depth shapes phytoplankton physiology, viral production, and accumulation in the North Atlantic. Nat Commun 12
39. Matsuta T et al (2024) Enhanced eddy activity along the Subantarctic Front under intensified westerly winds. Ocean Dyn 74:967–986

40. Shi F et al (2023) Contrasting trends in short-lived and long-lived mesoscale eddies in the Southern Ocean since the 1990s. Environ Res Lett 18:034042
41. He X et al (2025) Divergent hemispheric trends in marine dust deposition over the past two decades. Sci Bull
42. Jickells TD et al (2005) Global Iron Connections Between Desert Dust, Ocean Biogeochemistry, and Climate. Science 308:67–71
43. Dai Y et al (2023) Coastal phytoplankton blooms expand and intensify in the 21st century. Nature 615:280–284
44. Wei JW, Lee ZP, Shang SL (2016) A system to measure the data quality of spectral remote-sensing reflectance of aquatic environments. J Geophys Res -Oceans 121:8189–8207
45. Lee Z et al (2023) Absorption Coefficient and Chlorophyll Concentration of Oceanic Waters Estimated from Band Difference of Satellite-Measured Remote Sensing Reflectance. J Remote Sens 3:0063
46. Gregg WW, Casey NW (2007) Sampling biases in MODIS and SeaWiFS ocean chlorophyll data. Remote Sens Environ 111:25–35
47. He X, Stamnes K, Bai Y, Li W, Wang D (2018) Effects of Earth curvature on atmospheric correction for ocean color remote sensing. Remote Sens Environ 209:118–133
48. Robertson AR (1977) The CIE 1976 Color-Difference Formulae. Color Res Appl 2:7–11
49. Fairman HS, Brill MH, Hemmendinger H (1997) How the CIE 1931 color-matching functions were derived from Wright-Guild data. Color Res Appl 22:11–23
50. IOCCG (2000) Remote Sensing of Ocean Colour in Coastal, and Other Optically-Complex,Waters. IOCCG, Dartmouth, Canada
51. IOCGG (2006) Remote Sensing of Inherent Optical Properties: Fundamentals, Tests of Algorithms, and Applications. IOCCG, Dartmouth, Canada
52. Lee ZP, Carder KL, Arnone RA (2002) Deriving inherent optical properties from water color: a multiband quasi-analytical algorithm for optically deep waters. Appl Opt 41:5755–5772
53. Lee ZP, Arnone R, Hu CM, Werdell PJ, Lubac B (2010) Uncertainties of optical parameters and their propagations in an analytical ocean color inversion algorithm. Appl Opt 49:369–381
54. Mann HB (1945) Nonparametric Tests Against Trend. Econometrica 13:245–259
55. Sen PK (1968) Estimates of the regression coefficient based on Kendall's tau. J Am Stat Assoc 63:1379–1389
56. Hirsch RM, Slack JR, Smith RA (1982) Techniques of trend analysis for monthly water quality data. Water Resour Res 18:107–121
57. Shang S et al (2011) MODIS observed phytoplankton dynamics in the Taiwan Strait: an absorption-based analysis. Biogeosciences 8:841–850

Figures

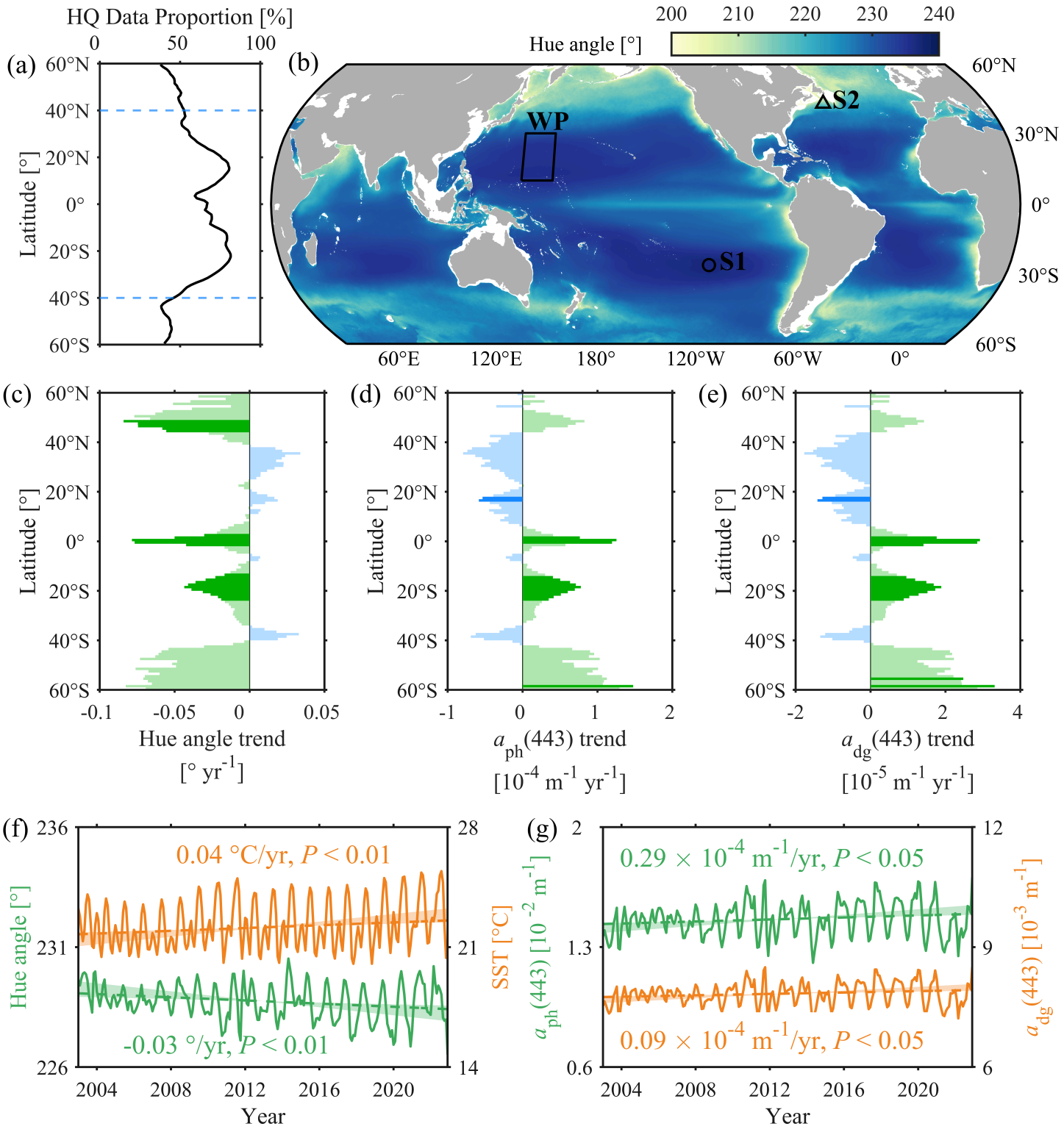


Figure 1

Latitudinal distributions, climatology, and temporal trends of ocean color metrics derived from the highest-quality (HQ) MODIS remote sensing reflectance data. a, Distribution of the HQ MODIS R_{rs} data between 60° S and 60° N. b, Hue angle climatology (2003–2022). c-e, Latitudinal trends (2003–2022) in annual mean hue angle (c), absorption coefficients at 443 nm of phytoplankton ($a_{ph}(443)$) (d), and nonliving materials ($a_{dg}(443)$) (e); f-g, Variability (2003–2022) of monthly spatial mean (60° S–60° N)

values for sea surface temperature (SST) and hue angle (f), and for $a_{ph}(443)$ *vs.* $a_{dg}(443)$ (g). All ocean color metrics are derived from the HQ MODIS R_{rs} dataset. In c–e, statistically significant trends ($P < 0.05$) are highlighted in dark colors. In f and g, dotted lines indicate long-term trends estimated by Sen's slope (Mann–Kendall test), with standard deviation represented by the shaded areas. Stations S1 & S2, and the black box in the western Pacific (WP), annotate the locations where satellite-derived remote sensing reflectance and *in situ* optical properties are presented (see Fig. S1).

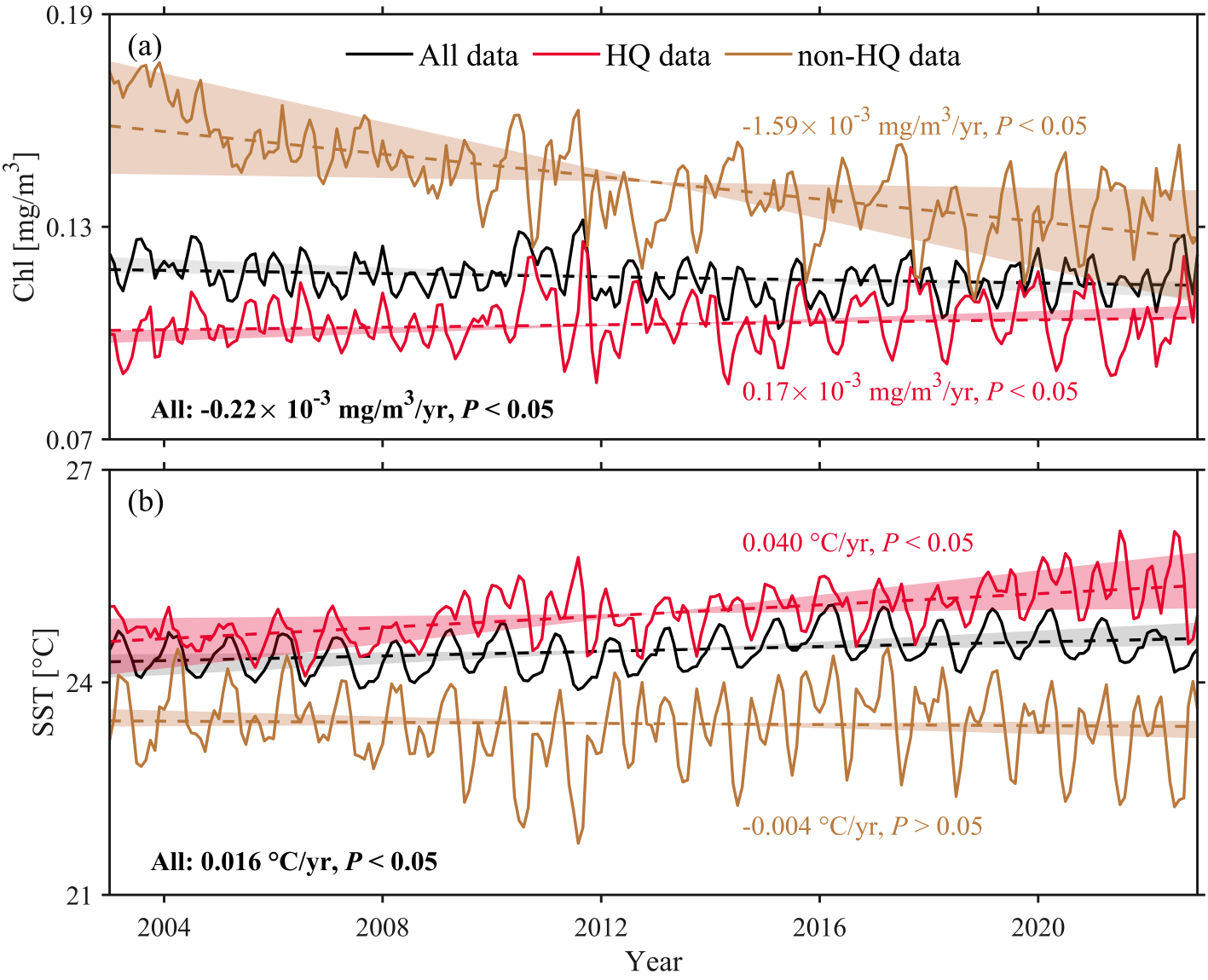


Figure 2

Variability of monthly mean chlorophyll-a concentration (Chl) derived from R_{rs} datasets of varying quality and its corresponding sea surface temperature (SST) in the ocean (40° S–40° N, 2003–2022). Chl from the highest-quality (HQ) R_{rs} (red), filtered non-HQ R_{rs} (brown), and the standard full dataset (black) (a), along with its corresponding SST (b).

Supplementary Files

This is a list of supplementary files associated with this preprint. Click to download.

- figureS1.png
- figureS2.png